Radiotherapy and Oncology 116 (2015) 94–99

Contents lists available at ScienceDirect

Radiotherapy and Oncology

journal homepage: www.thegreenjournal.com

Hypoxic PET

Feasibility and repeatability of PET with the hypoxia tracer [^{18}F]HX4 in oesophageal and pancreatic cancer

Remy Klaassen [a,b,*], Roelof J. Bennink [c], Geertjan van Tienhoven [d], Maarten F. Bijlsma [b], Marc G.H. Besselink [e], Mark I. van Berge Henegouwen [e], Johanna W. Wilmink [a], Aart J. Nederveen [f], Albert D. Windhorst [g], Maarten C.C.M. Hulshof [d], Hanneke W.M. van Laarhoven [a]

[a] Department of Medical Oncology; [b] LEXOR (Laboratory for Experimental Oncology and Radiobiology); [c] Department of Nuclear Medicine; [d] Department of Radiation Oncology; [e] Department of Surgery; [f] Department of Radiology, Academic Medical Center; and [g] Department of Radiology & Nuclear Medicine, VU University Medical Center, Amsterdam, The Netherlands

ARTICLE INFO

Article history:
Received 8 January 2015
Received in revised form 11 May 2015
Accepted 14 May 2015
Available online 3 June 2015

Keywords:
Hypoxia
Oesophageal cancer
Pancreatic cancer
[^{18}F]HX4 PET
Reproducibility

ABSTRACT

Background and purpose: To investigate the feasibility and to determine the repeatability of recurrent [^{18}F]HX4 PET scans in patients with oesophageal (EC) and pancreatic (PC) cancer.

Materials and methods: 32 patients were scanned in total; seven patients (4 EC/3 PC) were scanned 2, 3 and 4 h post injection (PI) of [^{18}F]HX4 and 25 patients (15 EC/10 PC) were scanned twice 3.5 h PI, on two separate days (median 4, range 1–9 days). Maximum tumour to background ratio (TBRmax) and the tumour hypoxic volume (HV) (TBR > 1.0) were calculated. Repeatability was assessed using Bland–Altman analysis. Agreement in localization was calculated as the distance between the centres of mass in the HVs.

Results: For EC, the TBRmax in the tumour (mean ± SD) was 1.87 ± 0.46 with a coefficient of repeatability (CoR) of 0.53 (28% of mean). The HV ranged from 3.4 to 98.8 ml with a CoR of 5.1 ml. For PC, the TBRmax was 1.72 ± 0.23 with a CoR of 0.27 (16% of mean). The HV ranged from 4.6 to 104.0 ml with a CoR of 7.8 ml. The distance between the centres of mass in the HV was 2.2 ± 1.3 mm for EC and 2.1 ± 1.5 mm for PC.

Conclusions: PET scanning with [^{18}F]HX4 was feasible in both EC and PC patients. Amount and location of elevated [^{18}F]HX4 uptake showed good repeatability, suggesting [^{18}F]HX4 PET could be a promising tool for radiation therapy planning and treatment response monitoring in EC and PC patients.

Oesophageal and pancreatic carcinomas are difficult to treat and have a very poor prognosis. (Chemo)radiotherapy plays a key role in both the curative and palliative treatment of these cancers [1,2]. Although these treatment regimens improve patient outcome, treatment response fluctuates greatly between patients and overall survival remains poor. For oesophageal cancer, complete response to neoadjuvant chemoradiation varies between 15% and 40% [3]. Studies investigating the efficacy of (radio)chemotherapy in patients with pancreatic ductal adenocarcinoma generally show an overall limited gain in median survival [4–6]. Oesophageal carcinomas have been associated with reduced oxygenation and resulting hypoxia related gene-expression [7]. The pancreatic tumour microenvironment is characterized by hypoxia, resulting from an abundance of stromal tissue and reduced vascularization [8–10]. Several studies have shown the relation of tumour hypoxia with adverse outcome in both oesophageal [11] and pancreatic cancer [12]. Hypoxia driven cell preserving pathways are associated with a more aggressive and metastatic tumour phenotype as well as resistance to chemotherapy and radiation [13–16]. The ionizing damage of radiation is increased by the formation of oxygen radicals. In hypoxic conditions the shortage of oxygen leads to a decreased effectiveness, and it is suggested that higher doses of radiation are needed to induce the same therapeutic effect, also known as the Oxygen Enhancement Ratio (OER) [17,18].

Reliable visualization of the distribution of hypoxic areas within the tumour may enable tailor made radiation therapy. Several techniques may deal with this: first, dose painting techniques may be used to increase the radiation dose to the hypoxic areas. Modern radiotherapy planning techniques as intensity modulated radiotherapy (IMRT), conformal arc techniques, tomotherapy and proton therapy can potentially enable selective delivery of a higher

* Corresponding author at: Department of Medical Oncology, Academic Medical Center, Meibergdreef 9, F0-209, 1105AZ Amsterdam, The Netherlands.
E-mail address: r.klaassen@amc.uva.nl (R. Klaassen).

http://dx.doi.org/10.1016/j.radonc.2015.05.009
0167-8140/

radiation dose solely to the more radio resistant, hypoxic, areas [19,20]. Second, radiation therapy or chemotherapy can be combined with various other modalities to enhance their effect on hypoxic tumours in case clinically relevant hypoxia is present. Options are the addition of carbogen breathing, radio-sensitizing agents as nimorazole or regional hyperthermia to enhance the effect of radiation or chemotherapy [21–23]. Furthermore, hypoxia activated pro-drugs as TH-302 can be used to specifically target hypoxic tumours [24,25]. Hypoxia PET imaging can be used to identify tumour hypoxia and could serve as a potential predictive marker to select those patients that would benefit from these hypoxia targeting treatment regimens [26–29].

2-nitroimidazole PET tracers have been developed to spatially identify and quantify hypoxic tumour areas. Due to the oxidation step involved in cell clearance, cell accumulation of 2-nitroamidazole derivatives is directly dependent on the intracellular pO_2 [30]. In recent years several 2-nitroimidazole derivatives have been developed and their ability to visualize in vivo tumour hypoxia has been studied in several tumour types [31,32].

[^{18}F]-3-Fluoro-2-(4-((2-nitro-1H-imidazol-1-yl)methyl)-1H-1,2,3-triazol-1-yl)propan-1-ol ([^{18}F]HX4, flortanidazole, Threshold Pharmaceuticals) is a relatively new 2-nitroimidazole derivative, which was developed to visualize hypoxic tumour areas. [^{18}F]HX4 may have a higher sensitivity, specificity and faster background clearance when compared in vivo to the most commonly used nitroimidazole hypoxia marker [^{18}F]FMISO. Earlier studies showed promising results using [^{18}F]HX4 as a hypoxia marker [33–37]. Similar tumour distribution was found for [^{18}F]HX4 and the most commonly used nitroimidazole hypoxia marker [^{18}F]FMISO in head and neck cancer [38]. Furthermore, both rat and mouse tumour models showed good correspondence of [^{18}F]HX4 tracer distribution with immunohistochemical stainings for hypoxia [33,39].

So far [^{18}F]HX4 has not been used to image hypoxia in oesophageal and pancreatic cancer. For future use in response evaluation and therapy guidance, a priori knowledge of variations in the measurements is important to distinguish treatment related effects from method related variations. Hence, knowledge of the repeatability of [^{18}F]HX4 PET scans is essential. The aim of this study was to investigate the feasibility to perform [^{18}F]HX4 PET in patients with oesophageal and pancreatic cancer and to determine the repeatability of repeated measures of [^{18}F]HX4 PET in these cancer types.

Materials and methods

Patients

Thirty-five patients with pathology proven oesophageal or pancreatic cancer were prospectively recruited. The study was approved by the medical ethics committee of the Academic Medical Center (University of Amsterdam) and informed consent was obtained from all individual participants included in the study. All scans were acquired before the start of initial cancer treatment.

[^{18}F]HX4 PET/CT

Imaging was performed on a GEMINI TF 16 PET/CT scanner (Philips Healthcare, Best, The Netherlands). Patients were scanned in supine position with their arms above their heads. A single bed position with an axial field of view of 18 cm was acquired of the primary tumour site for a total acquisition time of 15 min.

PET images were corrected for scatter and attenuation based on a low dose CT (LDCT) scan and reconstructed using a 3D ordered-subset iterative time-of-flight reconstruction algorithm with 3 iterations and 33 subsets. Resulting pixel spacing was 4×4 mm and 4 mm slice thickness with a spatial resolution of approximately 5 mm full width at half maximum (FWHM).

[^{18}F]HX4 was synthesized at the VU University Medical Center as described previously [33,35]. The injected dose was 434 ± 73 MBq based on an earlier performed phase 1 trial by van Loon et al. [35].

For protocol optimization, seven patients (4 oesophageal/3 pancreatic cancer) were scanned on one day, 2, 3 and 4 hours (h) post injection (PI) of [^{18}F]HX4. To investigate repeatability, 25 patients (15 oesophageal/10 pancreatic cancer) were scanned twice, on two separate days. Based on the results of the optimization study, showing only a minor increase in TBRmax between 3 and 4 h PI, and to be able to scan study patients directly following the clinical programme, patients in this group were scanned 3.5 h PI. Patients did not receive any further preparation instruction before the scans.

Image analysis

Repeated scans of the same patient were co-registered to match the first scan by maximizing the mutual information between the LDCT images, followed by an affine and b-spline registration in Elastix [40]. The corresponding PET images were then transformed according to the found parameters. After registration, the following volumes of interest (VOI) were drawn based on the LDCT: the tumour area in the oesophagus or pancreas and the aorta. Separately acquired diagnostic contrast enhanced CT images were used as reference for better tumour localization. The [^{18}F]HX4 PET scans were projected on the LDCT during VOI delineation, to make sure no activity spill from the liver or bile ducts was projected into the tumour VOIs.

Quantitative measures

Uptake concentrations were converted to standardized uptake values (SUV), correcting for injected dose and patient weight. Maximum tumour to background ratio (TBRmax) was calculated as the voxel with the maximum SUV value in the tumour VOI (SUVmax), divided by the average SUV of the voxels in the aorta VOI (SUVmean).

We defined the hypoxic volume (HV) as all voxels within the tumour VOI with TBR >1.0. This way all voxels with elevated [^{18}F]HX4 uptake compared to the blood pool are identified, whereas these voxels would be the most relevant for clinical practice. In addition, the HV was calculated for thresholds TBR >1.1 to TBR >1.4.

To evaluate correspondence in distribution of uptake intensity between the repeated scans, the voxels within this HV were used to calculate the centre of mass. The centre of mass was calculated by multiplying the activity of a voxel by its location in space for the x, y and z coordinate, divided by the total activity in the HV. In this way both the geometry of the HV and the distribution of [^{18}F]HX4 uptake are incorporated in one measure (see Fig. 1). The Euclidean distance between the centres of mass in the HV of the repeated scans was used to measure the repeatability in uptake distribution between the scans.

Statistical analysis

For statistical analysis the Prism 5.01 (GraphPad Software Inc., La Jolla, CA, USA) software package was used.

We used Wilcoxon signed rank test to calculate differences between, SUVmax, SUVmean, TBRmax on the 2 h, 3 h and 4 h Pi scans. Differences between SUVmax, SUVmean, TBRmax and HV between the scans on day 1 and 2 were also calculated using this

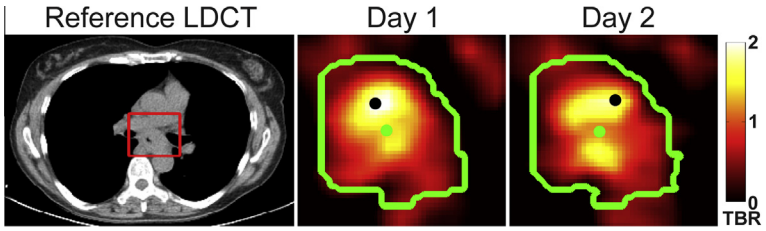

Fig. 1. 2D example of the Centre of Mass (green dot) of the area with TBR > 1.0 (green line) within the tumour ROI on day 1 and day 2 after registration. The black dot indicates the location of maximum intensity. On the left the LDCT on day 1 is shown with reference area (red box).

method. $p < 0.05$ was considered statistically significant. Results are given in mean ± standard deviation (SD).

To determine the repeatability of tumour SUVmax, TBRmax and HV, the methods described by Bland and Altman were used [41]. In the Bland–Altman plot the difference between the measurements on day 1 and 2 is plotted versus the average on both days. The coefficient of repeatability is calculated as 1.96 times the standard deviation of the difference between the paired measures. The lower and upper limit of agreement plotted in the Bland–Altman plot indicate the 95% confidence interval of normal variation in the measurements and are defined as the mean difference between the repeated measures minus or plus the coefficient of repeatability. Values outside the limits of agreement can be considered real biological changes, for instance indicating response to treatment. The repeatability index is defined as the coefficient of repeatability divided by the average of all repeated measurements times 100%.

Results

Data of thirty-two patients (5 females, 27 males) were available for further analysis (Table 1). Two patients did not complete the second repeatability scan, because the produced [18F] HX4 did not pass quality requirements. One patient did not show up for the second scan.

Mean age of the patient group was 60 ± 8 years (range 47–76 years). The optimization group consisted of 4 oesophageal cancer patients (1 squamous-cell carcinoma and 3 adenocarcinoma) and 3 patients with pancreatic ductal adenocarcinoma. The repeatability group consisted of 15 oesophageal cancer patients (3 squamous-cell carcinoma and 12 adenocarcinoma), and 10 patients with pancreatic ductal adenocarcinoma. All diagnoses were confirmed by pathological examination.

Due to technical issues, one 3 h PI scan failed. The remaining scans all showed good image quality. Mean SUVmax in the tumour VOI decreased slightly 2 h to 3 h (1.58 ± 0.38 to 1.35 ± 0.17, $p = 0.44$) and 3 h to 4 h PI (1.35 ± 0.17 to 1.27 ± 0.22, $p = 0.063$), resulting in a significant decrease from 2 h to 4 h PI (1.58 ± 0.38 to 1.27 ± 0.22, $p = 0.016$). SUVmean in the aorta VOI also decreased between 2 h and 4 h PI (1.12 ± 0.25 to 0.81 ± 0.21, $p = 0.016$). Overall the mean tumour TBRmax slightly increased in time from 1.50 ± 0.29 at 2 h PI, to 1.64 ± 0.39 at 3 h PI ($p = 0.16$), up to 1.67 ± 0.56 at 4 h PI ($p = 0.30$), although these differences were not statistically significant.

Median time between the two repeatability scans was 4 days (range 1–9 days). All repeated scans showed comparable image quality. Although 5 patients did receive a somewhat lower dose of [18F]HX4 in one of their repeated scans, this did not result in differences in image quality and analysis was performed as in all other repeated scans.

Typical examples of repeated [18F]HX4 scans in both a patient with oesophageal cancer and a patient with pancreatic cancer are shown in Fig. 2A.

Table 1
Patient characteristics.

	Patient	Age	Gender	Pathology	Stage
Oesophagus					
Optimization	EC1	54	M	SCC	T3N3M0
	EC2	65	M	AC	T3N2M0
	EC3	76	M	AC	T3N1M0
	EC4	67	M	AC	T3N1M0
Repeatability	EC5	61	M	AC	T3N0M1
	EC6	51	M	AC	T3N0M0
	EC7	53	M	AC	T3N1M0
	EC8	53	M	AC	T3N2M0
	EC9	55	M	AC	T3N1M0
	EC10	64	M	SCC	T3N2M0
	EC11	71	M	SCC	T2N2M0
	EC12	48	M	AC	T2N0M0
	EC13	60	M	AC	T3N2M0
	EC14	59	F	AC	T3N3M0
	EC15	55	M	AC	T3N2M0
	EC16	68	M	AC	T3N0M0
	EC17	61	M	AC	T3N1M0
	EC18	55	F	SCC	T3N3M0
	EC19	55	M	AC	T3N2M0
Pancreas					
Optimization	PC1	64	M	AC	T4N0M0
	PC2	53	M	AC	T4N0M0
	PC3	55	F	AC	T4N0M0
Repeatability	PC4	74	M	AC	T4N0M1
	PC5	53	M	AC	T4N1M1
	PC6	47	F	AC	T4N0M0
	PC7	60	M	AC	T4N1M1
	PC8	72	M	AC	T3N0M1
	PC9	59	M	AC	T3N1M1
	PC10	60	F	AC	T3N0M1
	PC11	74	M	AC	T4N0M1
	PC12	49	M	AC	T4N1M1
	PC13	70	M	AC	T3N0M0

EC*x*: oesophageal cancer. PC*x*: pancreatic cancer. SCC: squamous cell carcinoma, AC: adenocarcinoma.

Overall TBRmax for oesophageal cancer (1.87 ± 0.46) was slightly higher compared to pancreatic cancer (1.72 ± 0.23) for all scans. The HV (TBR > 1.0) ranged from 3.4 to 98.8 ml for oesophageal cancer and 4.6 to 104.0 ml for pancreatic cancer. For both oesophageal and pancreatic cancer, no significant differences were observed in aorta SUVmean, tumour SUVmax, TBRmax and HV between the scans on day 1 and day 2 (Table 2). The coefficient of repeatability for the TBRmax was 0.53 in oesophageal cancer and 0.27 in pancreatic cancer. Tumour TBRmax showed a slightly better repeatability index compared to SUVmax for both cancer types (Table 3). The Bland–Altman plots for TBRmax and HV for both cancer types are shown in Fig. 2B.

We did not observe an effect from the timing between the two repeated scans on the variation between the measurements. When dichotomized at the median interval of 4 days, separating the scans

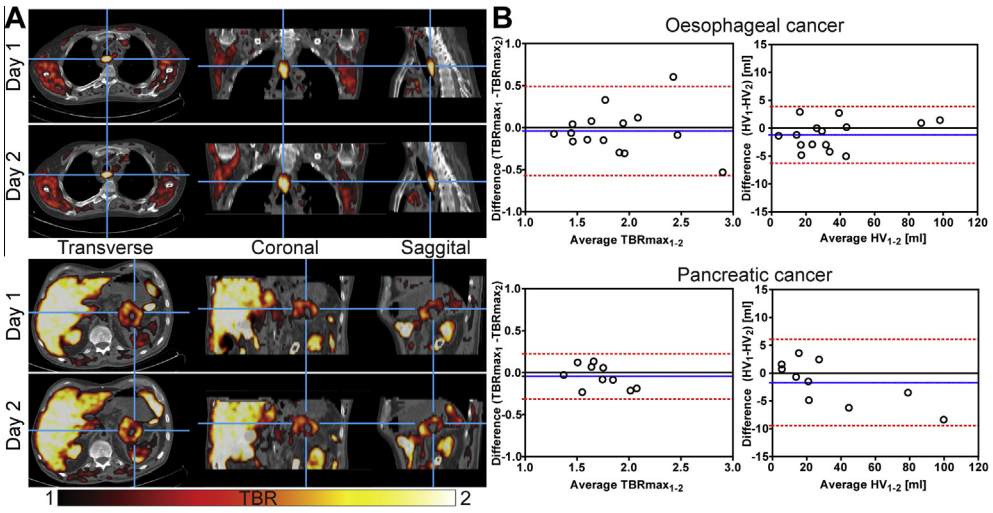

Fig. 2. (A) Typical [^{18}F]HX4 TBR images on day 1 and day 2 after registration, showing a patient with a squamous cell carcinoma in the mid oesophagus (top) and a patient with an adenocarcinoma in the tail of the pancreas (bottom), indicated by the crosshair. Physiological uptake of [^{18}F]HX4 is visible in the muscles, liver, kidneys and large intestine. (B) Bland–Altman plots showing the variation in TBR and HV (TBR > 1.0) between the repeated scans for both oesophageal and pancreatic cancer. The blue line indicates the mean difference and the red dashed lines indicate the limits of agreement.

Table 2
Parameters of the 2 repeated [^{18}F]HX4 PET studies for oesophageal and pancreatic cancer and the distance between the centres of mass of the tumour VOI.

Patient	Dose (MBq)		Tumour SUV_{max}		Aorta SUV_{mean}		TBR_{max}		HV (ml)		*D* (mm)
	1	2	1	2	1	2	1	2	1	2	
EC5	419	430	1.04	1.13	0.74	0.77	1.41	1.47	30.2	33.1	1.8
EC6	440	441	1.04	0.93	0.71	0.65	1.47	1.43	17.9	15.0	1.4
EC7	199	466	1.01	1.09	0.66	0.65	1.52	1.67	14.9	19.7	2.3
EC8	264	451	1.01	1.03	0.52	0.64	1.93	1.60	29.1	29.6	1.2
EC9	236	452	1.60	1.18	0.59	0.56	2.73	2.12	40.6	37.9	5.1
EC10	374	457	1.59	1.81	0.66	0.72	2.42	2.51	40.8	45.9	1.0
EC11	464	486	1.01	0.76	0.82	0.58	1.24	1.31	3.4	4.7	2.5
EC12	469	483	1.11	1.11	0.66	0.70	1.67	1.60	14.0	15.2	1.0
EC13	437	480	1.31	2.18	0.75	1.06	1.76	2.05	15.6	18.6	0.9
EC14	467	480	1.59	0.84	0.81	0.44	1.97	1.91	31.7	35.9	2.0
EC15	442	461	1.66	1.84	0.63	0.58	2.63	3.16	87.6	86.7	3.1
EC16	464	451	1.66	1.95	0.92	0.93	1.80	2.11	43.7	43.6	3.7
EC17	466	214	1.19	1.37	0.71	0.75	1.68	1.83	26.3	26.3	2.2
EC18	476	434	1.09	1.10	0.51	0.55	2.14	2.02	98.8	97.4	0.7
EC19	462	426	0.81	0.84	0.59	0.55	1.37	1.54	22.2	25.1	4.2
Mean	405	441	1.25	1.28	0.68	0.67	1.85	1.89	34.5	35.6	2.2
SD	94	66	0.29	0.37	0.11	0.11	0.46	0.48	26.5	25.6	1.3
p	NS ($p = 0.16$)		NS ($p = 0.39$)		NS ($p = 0.80$)		NS ($p = 0.36$)		NS ($p = 0.09$)		
PC4	470	442	1.53	1.70	0.77	0.79	1.98	2.17	77.2	80.7	1.0
PC5	453	484	1.34	1.26	0.80	0.79	1.67	1.60	41.4	47.7	1.1
PC6	388	475	1.41	1.29	0.90	0.89	1.57	1.45	20.2	21.6	1.7
PC7	474	448	1.59	1.58	0.88	0.84	1.80	1.89	95.6	104.0	1.0
PC8	489	486	1.52	1.82	0.89	1.02	1.70	1.79	5.9	5.2	2.6
PC9	475	487	1.41	1.33	0.74	0.63	1.91	2.12	13.5	14.2	4.5
PC10	456	456	1.42	1.44	0.82	0.90	1.73	1.59	18.8	23.7	4.8
PC11	456	445	1.27	1.30	0.89	0.78	1.43	1.67	17.2	13.6	1.5
PC12	458	440	0.96	0.58	0.54	0.34	1.78	1.72	28.4	25.9	0.6
PC13	441	461	1.13	0.76	0.83	0.55	1.36	1.39	6.2	4.6	2.7
Mean	456	462	1.36	1.31	0.81	0.75	1.69	1.74	32.4	34.1	2.1
SD	28	19	0.19	0.39	0.11	0.20	0.20	0.26	30.6	33.5	1.5
p	NS ($p = 0.82$)		NS ($p = 0.49$)		NS ($p = 0.19$)		NS ($p = 0.38$)		NS ($p = 0.38$)		

EC*x*: oesophageal cancer. PC*x*: pancreatic cancer. SUV: standardized uptake value. TBR: tumour to background ratio. *D*: distance between the centres of mass within the tumour hypoxic volumes (HV). SD: standard deviation. NS: non-significant ($p < 0.05$) with Wilcoxon signed rank test.

in two groups (interval > 4 days vs. interval < 4 days), there was no difference in variation between the groups.

The distance between the centres of mass in the HV on day 1 and 2 after registration was 2.2 ± 1.3 mm (range 0.7–5.1 mm) for oesophageal cancer and 2.1 ± 1.5 mm (range 0.6–4.8 mm) for pancreatic cancer, both falling within the FWHM of the scanner (approximately 5 mm).

Discussion

Hypoxia of tumours is of prognostic importance. In addition, it hampers the efficacy of treatments such as radiotherapy and chemotherapy. This treatment resistance may be overcome by adding hypoxia modifying drugs or hyperthermia or by irradiating the hypoxic areas with a higher dose [19–21,23,25]. Hence,

Table 3
Repeatability parameters of the 2 repeated [18F]HX4 PET studies for oesophageal (EC) and pancreatic (PC) cancer.

		Mean ± SD	Range	$Mean_{diff} \pm SD_{diff}$	CoR (RI)	CI
EC	SUV_{max}	1.26 ± 0.33	0.76–1.95	−0.03 ± 0.20	0.38 (30%)	−0.41–0.36
	TBR_{max}	1.87 ± 0.46	1.24–3.16	−0.04 ± 0.27	0.53 (28%)	−0.57–0.49
	HV (ml)	35.0 ± 25.6	3.4–98.8	−1.2 ± 2.6	5.1 (15%)	−6.3–3.9
PC	SUV_{max}	1.33 ± 0.30	0.58–1.82	0.05 ± 0.21	0.41 (31%)	−0.36–0.47
	TBR_{max}	1.72 ± 0.23	1.36–2.17	−0.04 ± 0.14	0.27 (16%)	−0.31–0.23
	HV (ml)	33.3 ± 31.2	4.6–104.0	−1.7 ± 4.0	7.8 (23%)	−9.4–6.1

SUV_{max}: Maximum Standardized Uptake Value. TBR_{max}: Maximum Tumour to Background Ratio. HV: Hypoxic Volume. $Mean_{diff}$ and SD_{diff}: Mean and standard deviation of the difference between scan 1 and scan2. CoR: Coefficient of Repeatability. RI: Repeatability Index. CI: 95% Confidence Interval of difference.

imaging of tumour hypoxia has potential value for therapy guidance. Furthermore, imaging of hypoxia may be used as a prognostic parameter and for response evaluation after radiochemotherapeutic treatment. The hypoxia marker flortanidazole [18F]HX4 is a potential candidate for imaging of hypoxia. However, the repeatability, and thus the quantifyability of this compound is mostly unknown. The aim of this study was to investigate the feasibility and determine the repeatability of [18F]HX4 PET scans in oesophageal and pancreatic cancer.

We found that image contrast and TBR was highest 4 h after injection of [18F]HX4. These findings are in accordance with earlier studies investigating image contrast at different time points PI of [18F]HX4 [33,36]. Although scanning at a later time point did not further increase TBR in a preclinical study [33], no patient studies investigating later time points than 4 h PI have been performed yet. The clinical implications of a longer accumulation period are not attractive, since it would require either a higher injected dose or longer acquisition time and a longer waiting period for the patient.

The Bland-Altman analysis of the TBRmax in our study showed that a normal variation of 28% in TBRmax can be expected for oesophageal cancer and 16% for pancreatic cancer. Thus, for monitoring of treatment response, effects must induce a greater change than this to be detectable. Studies investigating dynamics of hypoxic areas before and during (chemo)radiation suggest that hypoxia indeed changes in the course of treatment and moreover, residual hypoxia after the first courses of treatment has a higher prognostic value than baseline hypoxia [26,42–46]. The normal variation in [18F]HX4 uptake we found in this study was lower than the changes found during treatment, suggesting it to be able to assess these changes and thus as a potential tool for early response evaluation.

The number of studies investigating hypoxia PET in oesophageal and pancreatic cancer is limited. A study with 10 oesophageal squamous cell carcinomas showed great variations in tumour uptake and heterogeneity when [18F]FETNIM was used as a hypoxia tracer [47]. In contrast, our results showed more clustered areas of hypoxia, with good repeatability. Compared to an earlier in vivo study where [18F]FMISO hypoxia imaging was performed in pancreatic cancer, we observed higher image contrast and were better able to visually identify areas with increased tracer uptake [48]. This could well be explained by the longer time between injection and scanning (2 h vs. 3.5 h) and the faster background clearance of [18F]HX4 compared to [18F]FMISO [38].

In a study investigating the reproducibility of [18F]FMISO PET in 11 patients with head and neck cancer similar variations in TBR and HV were found as for [18F]HX4 in our study [49]. The repeatability we found for [18F]HX4 SUVmax in the current study is in the same range as the repeatability found for [18F]FDG PET, that has a normal variation of 25–30% [50]. However, it should be noted in the context of radiotherapy planning, that SUV based delineation of a volume is more challenging for low contrast tracers, like hypoxia tracers, compared to high contrast tracers as [18F]FDG.

Our results show that TBRmax was more stable in repeated scans than SUVmax. Furthermore, TBR images make it possible to apply a general threshold to visually identify hypoxic areas. For future use of [18F]HX4 in radiation planning, visualization of TBR, rather than the more regularly used SUV images, could help in a more robust delineation of hypoxic tumour areas. Future in vivo studies correlating histology derived parameters of hypoxia to [18F]HX4 uptake could provide the information necessary for quantitative interpretation of hypoxic areas (clinicaltrials.gov: NCT01989000). However, correlation with dedicated anatomical imaging is still needed for reliable tumour delineation.

The current approach in our study revealed several shortcomings, worthy of future investigation. First, we did not correlate [18F]HX4 uptake regions to local [18F]FDG uptake in this study, since only limited [18F]FDG scans were available in our study population. However, investigating this correlation might well be valuable for further tumour characterization, since [18F]FDG distribution is suggested to represent additional biological information compared to hypoxia tracers [51,52].

Second, we did not investigate the voxel-by-voxel correlation of [18F]HX4 uptake between the repeated scans. Due to lack of closely related bony features and lack of soft tissue contrast on the LDCT, image registration in the areas we investigated is more challenging compared to for instance the head and neck area. Although the registration of the LDCT scans showed good results, we therefore did not assume a one-on-one voxel correlation after registration. Furthermore, for radiation planning, regions of interest rather than separate voxels are used. Therefore, for radiation purposes clustered voxels showing elevated uptake are more important than per-voxel [18F]HX4 uptake. We therefore used distance between the centres of mass between elevated [18F]HX4 uptake as a more appropriate measure to compare uptake localization.

Last, both the oesophagus and pancreas are prone to respiratory motion. Organ motion during image acquisition will result in smear of the high intensity areas into wider areas of lower intensity, affecting SUV/TBRmax and consequently HV calculations. Correction for respiratory motion, e.g. by 4D acquisition, could be worthwhile for better identification of small hypoxic areas and a more accurate delineation of hypoxic regions.

In conclusion, we demonstrated the feasibility to perform [18F]HX4 PET imaging in both oesophageal and pancreatic cancer. Our results show that [18F]HX4 TBRmax and HV can be measured with good repeatability. This good agreement in location and size of regions with elevated [18F]HX4 uptake between repeated measures suggest [18F]HX4 PET could be a promising tool for response prediction as well as a more targeted approach in radiation planning.

Conflict of interest

The authors declare that they have no conflict of interest.

Appendix A. Supplementary data

Supplementary data associated with this article can be found, in the online version, at http://dx.doi.org/10.1016/j.radonc.2015.05.009.

References

[1] Stahl M, Mariette C, Haustermans K, Cervantes A, Arnold D. Oesophageal cancer: ESMO clinical practice guidelines for diagnosis, treatment and follow-up. Ann Oncol 2013;24.

[2] Seufferlein T, Bachet JB, Van cutsem E, Rougier P. Pancreatic adenocarcinoma: ESMO-ESDO clinical practice guidelines for diagnosis, treatment and follow-up. Ann Oncol 2012;23.

[3] Hingorani M, Crosby T, Maraveyas A, Dixit S, Bateman A, Roy R. Neoadjuvant chemoradiotherapy for resectable oesophageal and gastro-oesophageal junction cancer-do we need another randomised trial? Clin Oncol (R Coll Radiol) 2011;23:696–705.

[4] Antoniou G, Kountourakis P, Papadimitriou K, Vassiliou V, Papamichael D. Adjuvant therapy for resectable pancreatic adenocarcinoma: review of the current treatment approaches and future directions. Cancer Treat Rev 2014;40:78–85.

[5] Heinemann V, Haas M, Boeck S. Neoadjuvant treatment of borderline resectable and non-resectable pancreatic cancer. Ann Oncol 2013;24:2484–92.

[6] Rahma OE, Duffy A, Liewehr DJ, Steinberg SM, Greten TF. Second-line treatment in advanced pancreatic cancer: a comprehensive analysis of published clinical trials. Ann Oncol 2013;24:1972–9.

[7] Winther M, Alsner J, Tramm T, Nordsmark M. Hypoxia-regulated gene expression and prognosis in loco-regional gastroesophageal cancer. Acta Oncol 2013;52:1327–35.

[8] Mahadevan D, Von Hoff DD. Tumor-stroma interactions in pancreatic ductal adenocarcinoma. Mol Cancer Ther 2007;6:1186–97.

[9] Erkan M, Reiser-Erkan C, Michalski C. Cancer-stellate cell interactions perpetuate the hypoxia-fibrosis cycle in pancreatic ductal adenocarcinoma. Neoplasia 2009;11:497–508.

[10] Koong AC, Mehta VK, Le QT, Fisher GA, Terris DJ, Brown JM, et al. Pancreatic tumors show high levels of hypoxia. Int J Radiat Oncol Biol Phys 2000;48:919–22.

[11] Ping W, Sun W, Zu Y, Chen W, Fu X. Clinicopathological and prognostic significance of hypoxia-inducible factor-1alpha in esophageal squamous cell carcinoma: a meta-analysis. Tumour Biol 2014:4401–9.

[12] Kasuya K, Tsuchida A, Nagakawa Y, Suzuki M, Abe Y, Itoi T, et al. Hypoxia-inducible factor-1α expression and gemcitabine chemotherapy for pancreatic cancer. Oncol Rep 2011;26:1399–406.

[13] Brizel DM, Scully SP, Harrelson JM, Layfield LJ, Bean JM, Prosnitz LR, et al. Tumor oxygenation predicts for the likelihood of distant metastases in human soft tissue sarcoma. Cancer Res 1996;56:941–3.

[14] Höckel M, Knoop C, Schlenger K, Vorndran B, Baussmann E, Mitze M, et al. Intratumoral pO2 predicts survival in advanced cancer of the uterine cervix. Radiother Oncol 1993;26:45–50.

[15] Höckel M, Vaupel P. Tumor hypoxia: definitions and current clinical, biologic, and molecular aspects. J Natl Cancer Inst 2001;93:266–76.

[16] Saksø L, Busk M, Nordsmark M, Jakobsen S, Theil J, Overgaard J, et al. Accessing radiation response using hypoxia PET imaging and oxygen sensitive electrodes : A preclinical study 2011;99:418–23.

[17] Gray LH, Conger AD, Ebert M, Hornsey S, Scott OCA. The concentration of oxygen dissolved in tissues at the time of irradiation as a factor in radiotherapy. Br J Radiol 1953;26:638–48.

[18] Singers B, Busk M, Olthof N, Speel E, Horsman MR, Alsner J, et al. Radiosensitivity and effect of hypoxia in HPV positive head and neck cancer cells 2013;108:500–5.

[19] Servagi-Vernat S, Differding S, Sterpin E, Hanin F, Labar D, Bol A, et al. Hypoxia-guided adaptive radiation dose escalation in head and neck carcinoma: a planning study. Acta Oncol (Madr) 2015;1–9.

[20] Thorwarth D, Eschmann SM, Paulsen F, Alber M. Hypoxia dose painting by numbers: a planning study. Int J Radiat Oncol Biol Phys 2007;68:291–300.

[21] Henk J, Bischop K, Shepherd S. Treatment of head and neck cancer with CHART and nimorazole: phase II study. Radiother Oncol 2003;66:65–70.

[22] Overgaard J. Hypoxic modification of radiotherapy in squamous cell carcinoma of the head and neck – a systematic review and meta-analysis. Radiother Oncol 2011;100:22–32.

[23] Overgaard J. The heat is (still) on – the past and future of hyperthermic radiation oncology. Radiother Oncol 2013;109:185–7.

[24] Borad MJ. Randomized phase II trial of gemcitabine plus TH-302 versus gemcitabine in patients with advanced pancreatic Cancer. J Clin Oncol 2014;32:1–8.

[25] Wilson WR, Hay MP. Targeting hypoxia in cancer therapy. Nat Rev Cancer 2011;11:393–410.

[26] Mortensen LS, Johansen J, Kallehauge J, Primdahl H, Busk M, Lassen P, et al. FAZA PET/CT hypoxia imaging in patients with squamous cell carcinoma of the head and neck treated with radiotherapy: results from the DAHANCA 24 trial. Radiother Oncol 2012;105:14–20.

[27] Tran L, Bol A, Labar D, Cao-pham T, Jordan B, Grégoire V, et al. Predictive value of ^{18}F-FAZA PET imaging for guiding the association of radiotherapy with nimorazole: a preclinical study. Radiother Oncol 2015.

[28] Tran L-B-A, Bol A, Labar D, Karroum O, Bol V, Jordan B, et al. Potential role of hypoxia imaging using ^{18}F-FAZA PET to guide hypoxia-driven interventions (carbogen breathing or dose escalation) in radiation therapy. Radiother Oncol 2014;113:204–9.

[29] Horsman MR, Mortensen LS, Petersen JB, Busk M, Overgaard J. Imaging hypoxia to improve radiotherapy outcome. Nat Rev Clin Oncol 2012;9:674–87.

[30] Gagel B, Reinartz P, Dimartino E, Zimny M, Pinkawa M, Maneschi P, et al. pO(2) Polarography versus positron emission tomography ([(^{18})F] fluoromisonidazole, [(^{18})F]-2-fluoro-2′-deoxyglucose). An appraisal of radiotherapeutically relevant hypoxia. Strahlenther Onkol 2004;180:616–22.

[31] Krohn KA, Link JM, Mason RP. Molecular imaging of hypoxia. J Nucl Med 2008;49:129S–48S.

[32] Lopci E, Grassi I, Chiti A, Nanni C. PET radiopharmaceuticals for imaging of tumor hypoxia: a review of the evidence. Nucl Med Mol Imaging 2014;4:365–84.

[33] Dubois LJ, Lieuwes NG, Janssen MHM, Peeters WJM, Windhorst AD, Walsh JC, et al. Preclinical evaluation and validation of [^{18}F]HX4, a promising hypoxia marker for PET imaging. Proc Natl Acad Sci U S A 2011;108:14620–5.

[34] Doss M, Zhang JJ, Bélanger M-J, Stubbs JB, Hostetler ED, Alpaugh K, et al. Biodistribution and radiation dosimetry of the hypoxia marker 18F-HX4 in monkeys and humans determined by using whole-body PET/CT. Nucl Med Commun 2010;31:1016–24.

[35] Van Loon J, Janssen MHM, Ollers M, Aerts HJWL, Dubois L, Hochstenbag M, et al. PET imaging of hypoxia using [^{18}F]HX4: a phase I trial. Eur J Nucl Med Mol Imaging 2010;37:1663–8.

[36] Zegers CML, van Elmpt W, Wierts R, Reymen B, Sharifi H, Ollers MC, et al. Hypoxia imaging with [(18)F]HX4 PET in NSCLC patients: defining optimal imaging parameters. Radiother Oncol 2013;109:58–64.

[37] Peeters SGJ, Zegers CML, Lieuwes NG, van Elmpt W, Eriksson J, van Dongen GA, van Dongen GA, et al. A Comparative Study of the Hypoxia PET Tracers [^{18}F]HX4, [^{18}F]FAZA, and [^{18}F]FMISO in a Preclinical Tumor Model. Int J Radiat Oncol 2015;91:351–9.

[38] Chen L, Zhang Z, Kolb HC, Walsh JC, Zhang J, Guan Y. ^{18}F-HX4 hypoxia imaging with PET/CT in head and neck cancer: a comparison with ^{18}F-FMISO. Nucl Med Commun 2012;33:1096–102.

[39] Carlin S, Zhang H, Reese M, Ramos NN, Chen Q, Ricketts S-A. A comparison of the imaging characteristics and microregional distribution of 4 hypoxia PET tracers. J Nucl Med 2014;55:515–21.

[40] Klein S, Staring M, Murphy K, Viergever MA, Pluim JPW. Elastix: a toolbox for intensity-based medical image registration. IEEE Trans Med Imaging 2010;29:196–205.

[41] Bland JM, Altman DG. Statistical methods for assessing agreement between two methods of clinical measurement. Lancet 1986;1:307–10.

[42] Bollineni VR, Koole MJB, Pruim J, Brouwer CL, Wiegman EM, Groen HJM, et al. Dynamics of tumor hypoxia assessed by (18)F-FAZA PET/CT in head and neck and lung cancer patients during chemoradiation: possible implications for radiotherapy treatment planning strategies. Radiother Oncol 2014;113:198–203.

[43] Servagi-Vernat S, Differding S, Hanin F-X, Labar D, Bol A, Lee JA, et al. A prospective clinical study of (18) F-FAZA PET-CT hypoxia imaging in head and neck squamous cell carcinoma before and during radiation therapy. Eur J Nucl Med Mol Imaging 2014;41:1544–52.

[44] Yamane T, Kikuchi M, Shinohara S, Senda M. Reduction of [^{18}F]fluoromisonidazole uptake after neoadjuvant chemotherapy for head and neck squamous cell carcinoma. Mol Imaging Biol 2011;13:227–31.

[45] Tachibana I, Nishimura Y, Shibata T, Kanamori S, Nakamatsu K, Koike R, et al. A prospective clinical trial of tumor hypoxia imaging with ^{18}F-fluoromisonidazole positron emission tomography and computed tomography (f-miso pet/ct) before and during radiation therapy. J Radiat Res 2013;54:1078–84.

[46] Zips D, Zöphel K, Abolmaali N, Perrin R, Abramyuk A, Haase R, et al. Exploratory prospective trial of hypoxia-specific PET imaging during radiochemotherapy in patients with locally advanced head-and-neck cancer. Radiother Oncol 2012;105:21–8.

[47] Yue J, Yang Y, Cabrera AR, Sun X, Zhao S, Xie P, et al. Measuring tumor hypoxia with ^{18}F-FETNIM PET in esophageal squamous cell carcinoma: a pilot clinical study. Dis Esophagus 2012;25:54–61.

[48] Segard T, Robins PD, Yusoff IF, Ee H, Morandeau L, Campbell EM, et al. Detection of hypoxia with ^{18}F-fluoromisonidazole (^{18}F-FMISO) PET/CT in suspected or proven pancreatic cancer. Clin Nucl Med 2013;38:1–6.

[49] Okamoto S, Shiga T, Yasuda K, Ito YM, Magota K, Kasai K, et al. High reproducibility of tumor hypoxia evaluated by ^{18}F -fluoromisonidazole PET for head and neck cancer. J Nucl Med 2013;54:201–7.

[50] De Langen AJ, Vincent A, Velasquez LM, van Tinteren H, Boellaard R, Shankar LK, et al. Repeatability of ^{18}F-FDG uptake measurements in tumors: a metaanalysis. J Nucl Med 2012;53:701–8.

[51] Sato J, Kitagawa Y, Yamazaki Y, Hata H, Asaka T, Miyakoshi M, et al. Advantage of FMISO-PET over FDG-PET for predicting histological response to preoperative chemotherapy in patients with oral squamous cell carcinoma. Eur J Nucl Med Mol Imaging 2014;41:2031–41.

[52] Clausen M, Hansen A, Lundemann M, Hollensen C, Pommer T, Munck af Rosenschöld P, et al. Dose painting based on tumor uptake of Cu-ATSM and FDG: a comparative study. Radiat Oncol 2014;9:228.